Salvianolic acid B acts against non-small cell lung cancer A549 cells via inactivation of the MAPK and Smad2/3 signaling pathways

GUANGLEI HAN[1], YONGZHONG WANG[1], TONG LIU[2], JIARONG GAO[1], FENGYI DUAN[3], MING CHEN[4], YAN YANG[4] and CHAO WU[1]

Departments of [1]Pharmacy, [2]Respiratory Medicine, [3]Spleen and Stomach, The First Affiliated Hospital of Anhui University of Chinese Medicine, Hefei, Anhui 230031; [4]Department of Pharmacology, Anhui Medical University, Key Laboratory of Anti-Inflammatory and Immunopharmacology, Chinese Ministry of Education, Hefei, Anhui 230032, P.R. China

Received September 27, 2021; Accepted January 26, 2022

DOI: 10.3892/mmr.2022.12700

Abstract. Salvianolic acid B (Sal B) is a potential cytotoxic polyphenol against cancer. In the present study the effect of Sal B and its molecular mechanism were investigated in the non-small cell lung cancer (NSCLC) A549 cell line. The TGF-β/MAPK/Smad signaling axis was explored. A549 cells were co-cultured with and without different concentrations of Sal B (25, 50 and 100 μM respectively) and TGF-β_1 (9 pM) for 24 h. Cell epithelial-mesenchymal transition (EMT), cell migration, cell cycle distribution, autophagy and apoptosis were assessed by western blotting (WB), wound healing assay and flow cytometry, respectively. Moreover, activation of MAPK, Smad2/3 and the downstream target, plasminogen activator inhibitor 1 (PAI-1), were assessed by WB. The results demonstrated that Sal B inhibited TGF-β_1-induced EMT and migration of A549 cells, hampered cell cycle progression and induced cell autophagy and apoptosis. Furthermore, Sal B inactivated MAPK signaling pathways and the phosphorylation of Smad2/3, especially the phosphorylation of Smad3 at the linker region, which resulted in decreased protein expression levels of PAI-1 in TGF-β_1-stimulated A549 cells. Overall, these results demonstrated that Sal B may have a potential therapeutic effect against NSCLC *in vitro*. The results of the present study indicated that the underlying active mechanism of Sal B in NSCLC may be closely related to the impeded activation of the MAPK and Smad2/3 signaling pathways. Therefore, Sal B may be a potential candidate NSCLC therapeutic agent.

Correspondence to: Dr Chao Wu, Department of Pharmacy, The First Affiliated Hospital of Anhui University of Chinese Medicine, 117 Meishan Road, Hefei, Anhui 230031, P.R. China
E-mail: hfwuchao2015@sohu.com

Professor Yan Yang, Department of Pharmacology, Anhui Medical University, Key Laboratory of Anti-Inflammatory and Immunopharmacology, Chinese Ministry of Education, 81 Meishan Road, Hefei, Anhui 230032, P.R. China
E-mail: yangyan@ahmu.edu.cn

Key words: non-small cell lung cancer, salvianolic acid B, TGF-β, Smad2/3, MAPK

Introduction

Lung cancer is one of the most commonly diagnosed malignancies and one of the main causes of cancer-related deaths worldwide (1). In 2018, 2.09 million new cases and 1.76 million deaths were estimated to be attributed to lung cancer, as determined using the Global Cancer Incidence, Mortality and Prevalence database (1). The morbidity and mortality rates of lung cancer have also shown an annual increase (1). Non-small cell lung cancer (NSCLC), the dominant type of lung cancer, represents ~85% of total lung cancer cases (2). The main subtypes of NSCLC are lung adenocarcinoma and lung squamous cell carcinoma (2). At present, advancements in the treatment of NSCLC, including small-molecule tyrosine kinase inhibitors (TKIs) and immunotherapy, have increased patient survival rates in certain patients (2). However, the overall survival rate of patients with NSCLC remains low, especially in patients with metastatic NSCLC (2). Traditional Chinese medicine (TCM) in the adjuvant therapy in patients with NSCLC is considered to have potential therapeutic value in improving prognosis (3).

In TCM, *Salvia miltiorrhiza* Bunge (SM) is used to treat numerous diseases, including various cancer types, based on its efficacy in promoting circulation and removing stasis (4). The activity of SM is a result of lipophilic compounds, including tanshinones and cryptotanshinones, and hydrophilic phenolic acids, including salvianolic acid A (Sal A) and salvianolic acid B (Sal B) (5). Sal B has the highest content of the aforementioned compounds in SM. It has been reported to be a potential cytotoxic polyphenol and is therefore a potential therapeutic in a number of different cancers, including, hepatocellular carcinoma, breast cancer, head and neck squamous cell carcinoma, gastric cancer and colorectal cancer, based on laboratory data (6-11). Furthermore, Sal B was observed to inhibit NSCLC A549 cell growth; its half maximal inhibitory

concentration (IC_{50}) value was determined to be a concentration of 279.6 μM (12). A previous study suggested that Sal B is also likely to be a potential therapeutic candidate for NSCLC (12). However, the use of Sal B for NSCLC treatment has not yet been adequately elucidated, and the molecular mechanisms of the anti-NSCLC activities of Sal B remain unclear.

Epithelial-mesenchymal transition (EMT) is a cell phenotype transformation process, which is a crucial patho-mechanism for enhanced tumorigenesis and metastasis, contributing to the malignant progression of cancer (13). Transforming growth factor β_1 (TGF-β_1), a common pluripotential cytokine, induces EMT and therefore contributes to tumor invasion and metastasis, inhibiting apoptotic stimuli in various cancer cells including NSCLC (14). Inhibition of TGF-β signaling is a novel and effective strategy for NSCLC therapy (15). Sal B has been reported to serve an important role in anti-pulmonary fibrosis via inhibition of the TGF-β signaling pathway, which suggests that suppression of TGF-β signaling could be a crucial mechanism in the biological activity of Sal B (16). It can therefore be hypothesized that Sal B has a therapeutic effect in NSCLC via inhibition of the TGF-β signaling pathway. In the present study, TGF-β_1-stimulated NSCLC A549 cells were employed and co-cultured with different concentrations of Sal B. Changes in cell function and the intracellular mechanism of the TGF-β signaling pathway were detected.

Materials and methods

Drugs and reagents. Sal B (chemical abstracts service no. 115939-25-8; molecular formula, $C_{36}H_{30}O_{16}$; molecular weight, 718.61 Da; the chemical structure is displayed in Fig. 1) was purchased from Nantong FeiYu Biotechnology Co., Ltd. with a purity of >98% (cat. no. FY1167B013). Recombinant human TGF-β_1 (cat. no. 100-21) was purchased from PeproTech, Inc. The Cell Cycle Detection kit (cat. no. BB-4104-2) and BBcellProbe™ Annexin V-FITC Double-staining Cell Apoptosis Detection kit (cat. no. BB-4101-2) were obtained from BestBio Co. Cell lysis buffer for western blotting (cat. no. P0013) and phenylmethylsulfonyl fluoride (PMSF) (cat. no. ST506) were purchased from the Beyotime Institute of Biotechnology. The following primary antibodies were used in the present study: rabbit polyclonal anti-E-cadherin (cat. no. WL01482), anti-N-cadherin (cat. no. WL01047), anti-vimentin (cat. no. WL01960), anti-Snail (cat. no. WL01960), anti-cyclin B1 (cat. no. WL01760), anti-cyclin-dependent kinase inhibitor 1 (p21)/WAF1 (cat. no. WL0362), anti-LC3α/β (cat. no. WL01506), anti-p62 (cat. no. WL02385), anti-Beclin1 (cat. no. WL02508), anti-Bax (cat. no. WL01637), anti-Bcl-2 (cat. no. WL01556), anti-caspase-3/cleaved-caspase-3 (cat. no. WL02117), anti-phosphorylated (p)-ERK1/2 (Thr^{202}/Thr^{204}; cat. no. WLP1512), anti-ERK1/2 (cat. no. WL01864), anti-p-JNK1/2 (Thr^{183}/Tyr^{185}; cat. no. WL01813), anti-JNK1/2 (cat. no. WL01295), anti-p-p38 (Thr^{180}/Thr^{182}; cat. no. WLP1576), anti-p38 (cat. no. WL00764), anti-p-Smad2 (Ser^{465}/Ser^{467})/p-Smad3 (Ser^{423}/Ser^{425}; cat. no. WL02305), anti-Smad2/3 (cat. no. WL01520), anti-plasminogen activator inhibitor-1 (PAI-1; cat. no. WL01486) and anti-GAPDH (cat. no. WL03412) antibodies were acquired from Wanleibio Co. Ltd. Anti-p-Smad3 linker region (Ser^{208}/Ser^{213}, p-Smad3L; cat. no. 28029) was purchased from Immuno-Biological Laboratories Co., Ltd. The secondary antibody, HRP-conjugated goat anti-rabbit IgG (heavy chain + light chain; cat. no. ZB-2301) was obtained from OriGene Technologies, Inc. ECL Plus Western Blotting Substrate (cat. no. C05-07004) was purchased from BIOSS.

Cell culture. The human NSCLC A549 cell line was purchased from the American Type Culture Collection (ATCC). A549 cells were cultured as a sub-confluent monolayer in RPMI-1640 medium (cat. no. SH30809.01; Hyclone; Cytiva) containing 10% FBS (cat. no. 11011-8611; Hangzhou Sijiqing Biological Engineering Materials Co., Ltd.), penicillin (100 U/ml)/streptomycin (0.1 mg/ml; cat. no. C0222; Beyotime Institute of Biotechnology) in a humidified incubator with sterile air containing 5% CO_2 at 37˚C. Cells in the logarithmic growth phase were routinely cultured for 24 h after being plated and were subsequently used in the following experiments. All experiments were performed in triplicate.

Cell migration assay. The effect of Sal B on A549 cell migration was visualized using the wound healing assay. Cells in the logarithmic growth phase were digested using trypsin-EDTA solution (cat. no. C0201; Beyotime Institute of Biotechnology) and were subsequently collected, counted and reseeded into a sterile 6-well plate ($1x10^6$ cells/well). These cells were cultured in RPMI-1640 medium containing 10% FBS. When these cells reached almost 100% confluency, serum-free RPMI-1640 medium was used for 12 h to synchronize cell growth. Scratches were made on the inner surface of the 6-well plates using a sterile 200-μl pipette tip. Subsequently, these cells were washed using PBS and cultured in serum-free RPMI-1640 medium with or without Sal B (25, 50 and 100 μM) and TGF-β_1 (9 pM) for 24 h (37˚C, 5% CO_2). Representative images were captured using an inverted microscope (x100 magnification; CKX53; Olympus Corporation) at 0, 12 and 24 h. The width of the scratch area was also measured, and the healing rate of the scratch (%) was quantified using the following formula: Healing rate of scratch (%) = (the width of scratch area at 0 h-the width of scratch area at 12/24 h)/the width of scratch area at 0 h x100% (17).

Cell cycle detection. The effect of Sal B on the cell cycle in A549 cells was detected using flow cytometry (FCM). Briefly, logarithmic growth phase A549 cells were collected, counted and reseeded in a sterile 6-well plate to a density of $5x10^5$ cells/well. Cells were cultured in RPMI-1640 medium containing 10% FBS. Once the cells reached 90% confluency they were synchronized by culturing in serum-free RPMI-1640 medium for 12 h (37˚C, 5% CO_2). Subsequently, concentration-graded Sal B (25, 50 and 100 μM) and/or TGF-β_1 (9 pM) were added to serum-free medium and cells were incubated for 24 h (37˚C, 5% CO_2). After culturing, the cells were collected and washed using cooled PBS twice. Cells were fixed using cooled 70% ethanol at 4˚C overnight. On the following day, the cells were resuspended in 300 μl cooled PBS following washing. RNase A solution (20 μl/sample) was added and these cells were incubated at 37˚C for 30 min. Subsequently, the cells were stained with propidium iodide (PI) solution (400 μl/sample) at 4˚C for 1 h in the dark. The cell

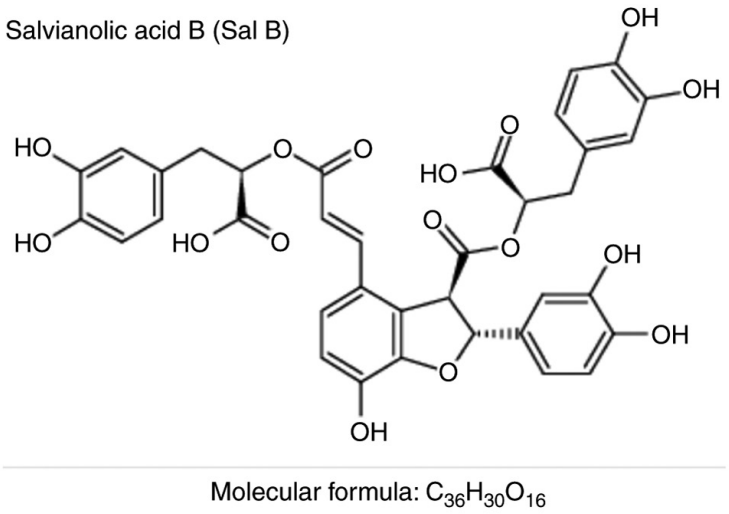

Figure 1. Chemical structure of Salvianolic acid B (Sal B).

cycle distribution was determined using a BD FACSCelesta™ flow cytometer (BD Biosciences). These results were analyzed using FlowJo 7.6.1 software (BD Biosciences).

Cell apoptosis detection. The apoptotic rate was evaluated using the BBcellProbe™ Annexin V-FITC Double-staining Cell Apoptosis Detection kit according to the manufacturer's protocol. Briefly, A549 cells in the logarithmic phase were collected, counted and seeded into a sterile 6-well plate ($5x10^5$ cells/well). Subsequently, these cells were treated with Sal B (25, 50 and 100 μM) and TGF-β_1 (9 pM) for 24 h (37˚C, 5% CO_2). Following treatment, these cells were collected and washed with pre-cooled PBS twice and then suspended in 1X Annexin V binding buffer (400 μl/sample). Annexin V-FITC (5 μl/sample) was added and the cells were incubated at 4˚C for 15 min in the dark. PI staining-solution (5 μl/sample) was added and these cells were re-incubated at 4˚C for 5 min in the dark. Cell apoptosis in each sample was analyzed using the BD FACSCelesta™ flow cytometer. These data were quantified using FlowJo 7.6.1 software.

Extraction of total cell protein and western blotting. A549 cells were treated with Sal B (25, 50 and 100 μM) and TGF-β_1 (9 pM) for 24 h (37˚C, 5% CO_2). Following treatment, total protein was extracted from the cells using cell lysis buffer for western blotting containing a proteinase inhibitor, PMSF (1 mM), according to the manufacturer's protocol. Protein expression levels were detected via western blotting as previously described (18). In brief, proteins (50 μg/sample) were separated using 10% SDS-PAGE and the separated proteins were transferred to a PVDF membrane (MilliporeSigma). Membranes were blocked using 5% skimmed milk powder (room temperature, 2 h). Subsequently, the membranes were incubated with the following primary antibodies (4˚C overnight): rabbit anti-N-cadherin (1:1,000), anti-vimentin (1:500), anti-Snail (1:1,000), anti-E-cadherin (1:1,000), anti-cyclin B1 (1:1,000), anti-p21/WAF1 (1:1,000), anti-LC3α/β (1:1,000), anti-p62 (1:500), anti-Beclin1 (1:1,000), anti-Bax (1:1,000), anti-Bcl-2 (1:500), anti-caspase-3/cleaved-caspase-3 (1:500), anti-p-ERK1/2 (1:300), anti-ERK1/2 (1:500), anti-p-JNK1/2 (1:1,000), anti-JNK1/2 (1:1,000), anti-p-p38 (1:1,000), anti-p38 (1:1,000), anti-p-Smad2/3 (1:1,000), anti-p-Smad3L (1:1,000), anti-Smad2/3 (1:1,000), anti-PAI-1 (1:1,000) and anti-GAPDH (1:1,000). Following primary incubation, the membranes were incubated with goat anti-rabbit IgG-HRP antibody (1:10,000). Protein bands were visualized using ECL Plus Western Blotting Substrate under the UVP ChemiStudio Imaging System (Analytik Jena GmbH). Densitometric analysis of the protein bands was performed using ImageJ 2.x software (National Institutes of Health). GAPDH was used as the internal reference gene. The ratio of semi-quantified protein to GAPDH in the control group was assigned a value of 1.

Statistical analysis. Data are presented as the mean ± SD. Statistical analyses were performed using SPSS 16.0 software for Windows (SPSS, Inc.). Pairwise comparison of multiple group means were determined using a one-way ANOVA followed by Tukey's multiple comparison test. $P<0.05$ was considered to indicate a statistically significant difference.

Results

Sal B inhibits the TGF-β_1-induced EMT and cell migration in A549 cells. EMT-inducing factors, including the TGF-β family, contribute to tumor cell malignant transformation, which results in enhanced metastasis (19). Therefore, the effect of Sal B on TGF-β_1-induced EMT and migration of human NSCLC A549 cells was investigated. The results demonstrated that important marker proteins in EMT, including N-cadherin, vimentin and Snail, presented with increased protein expression levels in A549 cells following TGF-β_1 stimulation, whereas co-treatment with three different concentrations of Sal B with TGF-β_1 resulted in a significant dose-dependent decrease in these aforementioned protein expression levels (Fig. 2A). E-cadherin, a protective protein that inhibits the EMT, was observed to increase in a dose-dependent manner in Sal B-treated A549 cells compared with those cells treated with TGF-β_1 only (Fig. 2A). Moreover, the migration of A549 cells was enhanced by

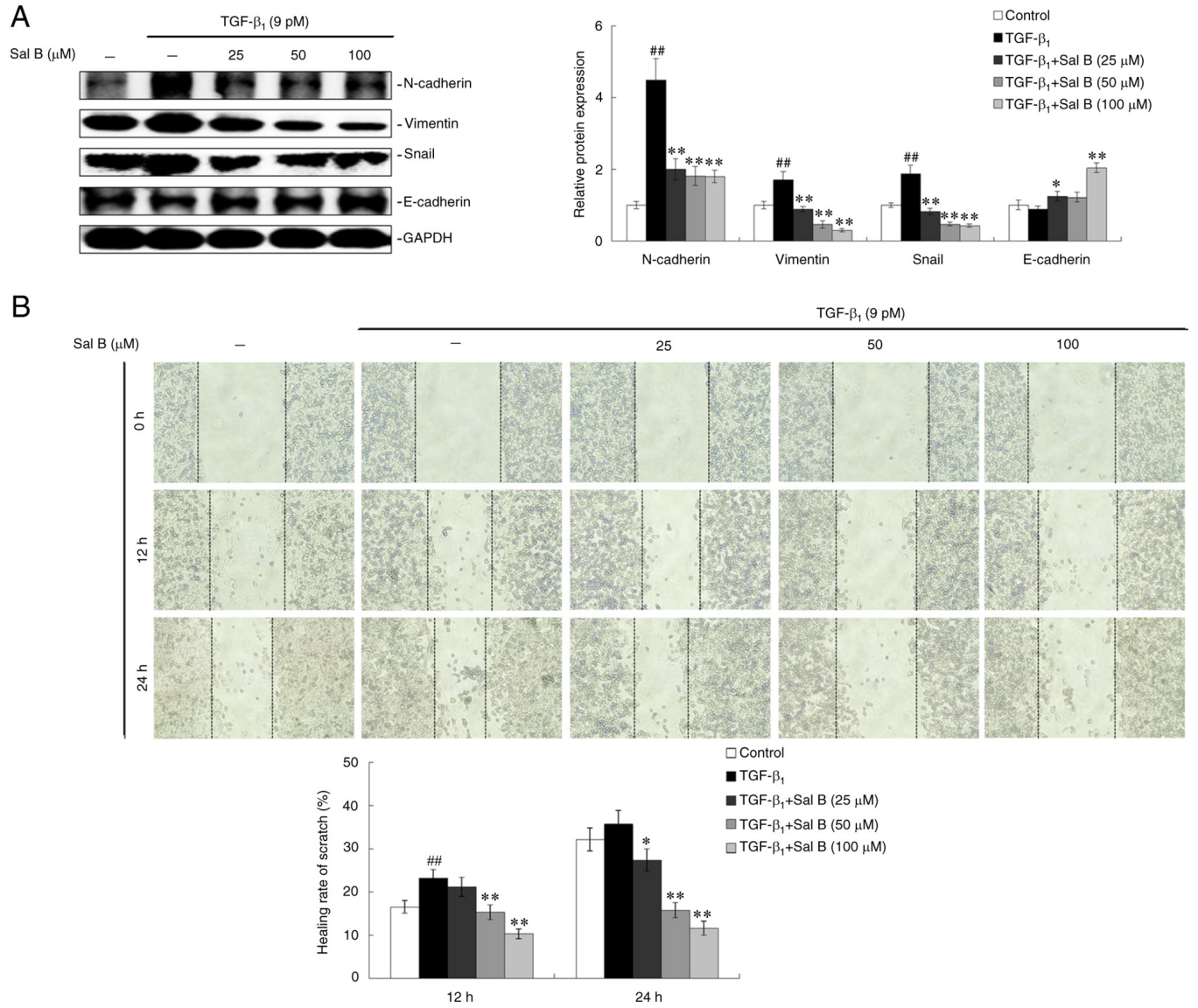

Figure 2. Effects of Sal B on EMT and cell migration induced by TGF-β_1 in A549 cells. (A) Protein expression levels of EMT marker proteins, N-cadherin, Vimentin, Snail and E-cadherin, were analyzed via western blotting. (B) Cell migration was assessed using a wound healing assay. $^{\#\#}$P<0.01 vs. the control; *P<0.05, **P<0.01 vs. the TGF-β_1 only-stimulated group. Sal B, salvianolic acid B; EMT, epithelial-mesenchymal transition; TGF-β_1, transforming growth factor β_1.

TGF-β_1 treatment, whereas Sal B co-treatment resulted in a dose-dependent inhibitory effect on TGF-β_1-induced cell migration at 12 and 24 h (Fig. 2B).

Sal B inhibits the cell cycle progression of TGF-β_1-stimulated A549 cells. Vigorous cell proliferation reflected by rapid cell division is a typical characteristic of cancer cells (20). Whether Sal B induces NSCLC cell cycle arrest, resulting in the inhibition of the proliferation of TGF-β_1-stimulated A549 cells, was therefore investigated. A decreased percentage of A549 cells in the G_0/G_1 phase and an increased percentage of cells in the S and G_2/M phase under TGF-β_1 stimulation were observed, compared with the control group. Co-treatment with Sal B and TGF-β_1 induced G_0/G_1 phase arrest in A549 cells (Fig. 3A). Cyclin B1 and p21/WAF1 (p21) are crucial for cell cycle progression; p21 promotes cyclin B1 proteasomal degradation to contribute to arrest of the cell cycle (21). The results demonstrated increased protein expression levels of cyclin B1 and decreased p21 protein expression levels in A549 cells induced by TGF-β_1. However, co-treatment with Sal B resulted in inhibition of the TGF-β_1-induced elevation of cyclin B1 and reduction in p21 (Fig. 3B).

Sal B induces the autophagy of TGF-β_1-stimulated A549 cells. Autophagy inhibition is a common phenomenon in numerous types of cancer cells including NSCLC (22). The effect of Sal B on NSCLC cell autophagy in TGF-β_1-stimulated A549 cells was therefore investigated. A few important marker proteins of autophagy were assessed. The results demonstrated that LC3α exhibited reduced protein expression levels, whereas increased protein expression levels were displayed by LC3β in the TGF-β_1-stimulated A549 cells when treated with concentration-graded Sal B, especially in the 100 μM Sal B-treatment group. TGF-β_1 increased the protein expression levels of p62 whereas Beclin1 protein expression levels were decreased, which were reversed by combined treatment

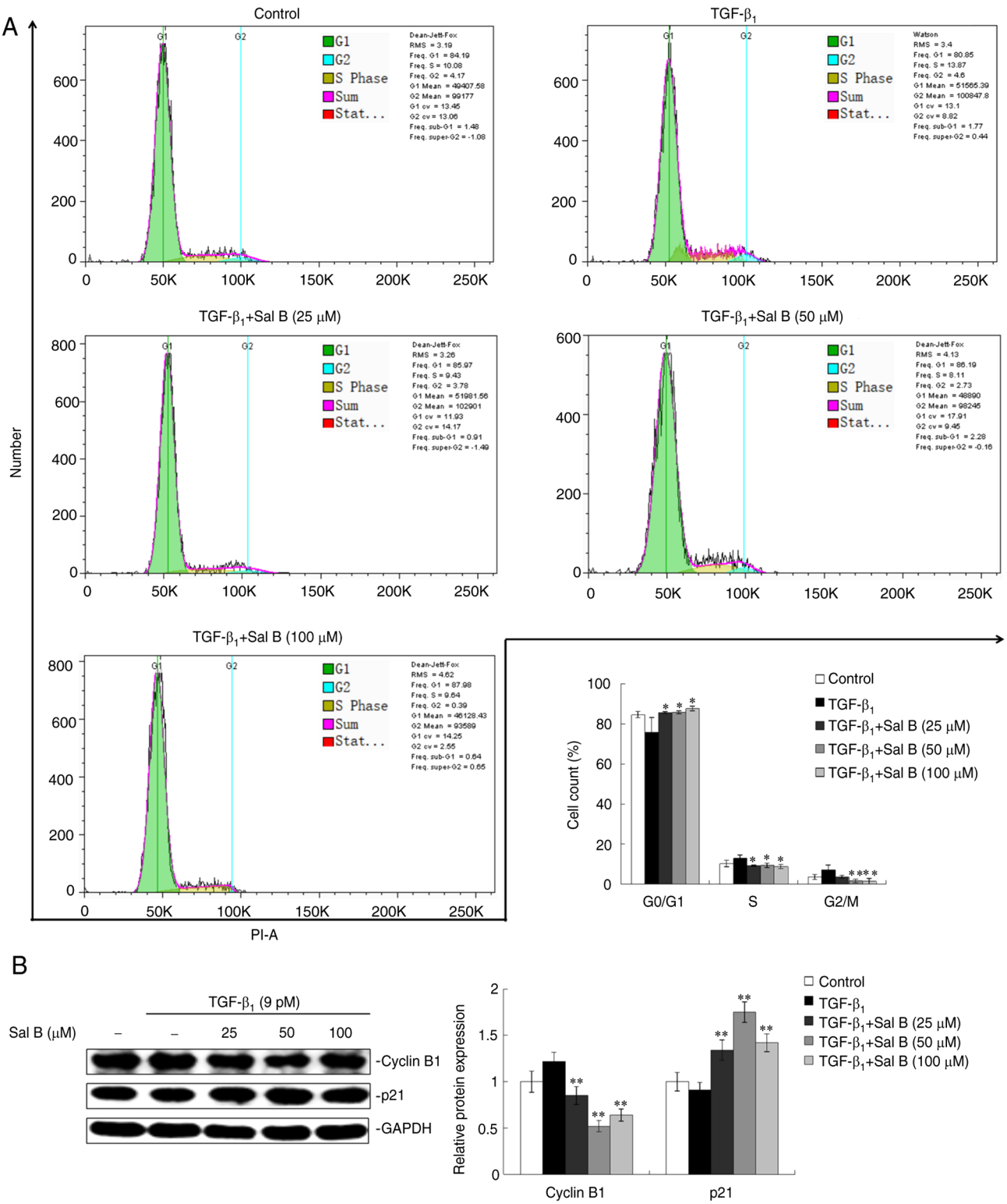

Figure 3. Effects of Sal B on cell cycle progression in TGF-β_1-stimulated A549 cells. (A) Cell cycle distribution of A549 cells following treatment was detected using a cell cycle detection kit. (B) Protein expression levels of two important communicators in cell cycle progression, cyclin B1 and p21, were assessed via western blotting. *P<0.05, **P<0.01 vs. the TGF-β_1 only-stimulated group. Sal B, salvianolic acid B; p21, cyclin-dependent inhibitor kinase 1; TGF-β_1, transforming growth factor β_1.

with concentration-graded Sal B. The most obvious change was observed for p62 (Fig. 4).

Sal B induces apoptosis in TGF-β_1-stimulated A549 cells. Inducing cell apoptosis is a major strategy in cancer treatment (23). Therefore the effect of Sal B on NSCLC cell apoptosis was examined via FCM, which was used to quantify crucial marker proteins. The results demonstrated that a repressed apoptotic rate was observed in A549 cells under TGF-β_1-stimulation alone, whereas co-treatment with Sal B

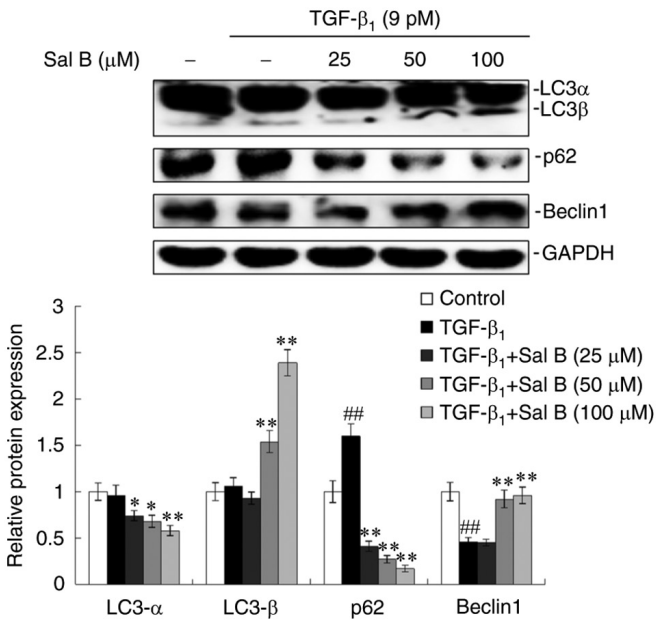

Figure 4. Effects of Sal B on cell autophagy in TGF-β_1-stimulated A549 cells. Protein expression levels of important marker proteins of autophagy, including LC3α/β, p62 and Beclin1 were assessed via western blotting. ##P<0.01 vs. the control; *P<0.05, **P<0.01 vs. the TGF-β_1 only-stimulated group. Sal B, salvianolic acid B; TGF-β_1, transforming growth factor β_1.

resulted in the induction of apoptosis in A549 cells. Increased apoptotic rates were demonstrated at all three Sal B concentrations compared with the TGF-β_1-stimulated only group (Fig. 5A). Investigation of crucial apoptotic marker protein expression levels demonstrated that TGF-β_1 had an inhibitory effects on Bax, caspase-3 and cleaved-caspase-3, but had a stimulative effect on Bcl-2 protein expression levels. Co-treatment using three different concentrations of Sal B reversed these effects caused by TGF-β_1 treatment (Fig. 5B).

Sal B inactivates the MAPK signaling pathway in TGF-β_1-stimulated A549 cells. MAPK signaling pathways are regarded as noncanonical TGF-β signaling pathways and serve an important role in the cytological effects mediated by TGF-β_1 (24). Therefore, the activation of MAPK signaling pathways in TGF-β_1-stimulated A549 cells under Sal B treatment was investigated. The activation of MAPK signaling pathways can be assessed using the phosphorylation levels of the following three crucial MAPKs: ERK1/2, JNK1/2 and p38. It was observed that TGF-β_1 induced increased protein expression levels of p-ERK1/2, p-JNK1/2 and p-p38, whereas co-treatment with Sal B resulted in the dose-dependent inhibition of ERK1/2, JNK1/2 and p38 phosphorylation. Furthermore, significantly inhibited protein expression levels of ERK1/2 were observed under Sal B co-treatment in TGF-β_1-stimulated A549 cells at 24 h (Fig. 6).

Sal B inhibits the phosphorylation of Smad2/3 and PAI-1 expression in TGF-β_1-stimulated A549 cells. Smad2/3 is regarded as the main intracellular effector of canonical TGF-β signal transduction, which is phosphorylated and nuclear-translocated to regulate target genes, such as PAI-1, as a transcription factor (25). The results demonstrated that p-Smad2 protein expression levels were significantly increased in A549 cells following TGF-β_1 stimulation for 24 h. However, respective co-treatment with three different concentrations of Sal B led to reduced p-Smad2 and p-Smad3 protein expression levels, compared with those with TGF-β_1 treatment only. MAPK-mediated Smad3 phosphorylation at the linker region serves an important role in TGF-β signaling and exerts a carcinogenic effect (26). The results demonstrated that the protein expression levels of p-Smad3L were significantly reduced under Sal B treatment in TGF-β_1-stimulated A549 cells (Fig. 7). An important target, PAI-1, of the TGF-β/Smad signaling pathway displayed increased protein expression levels in A549 cells under TGF-β_1 stimulation for 24 h, which were subsequently inhibited with Sal B co-treatment in a dose-dependent manner (Fig. 7).

Discussion

Natural polyphenols are potential active ingredients for the prevention and treatment of cancer (27). Phenolic acids [including salvianolic acid A (Sal A) and Sal B] from *Salvia miltiorrhiza* Bunge (SM), one of the major polyphenol classes, have been reported for their therapeutic properties against cancer in various solid tumors (11). Sal A has been experimentally verified to inhibit cell growth and induce partial apoptosis (28), and reverse cisplatin resistance in human non-small cell lung cancer (NSCLC) A549 cells (29). Sal B and Sal A have both structural and functional similarities (11). Related research has shown that the percentage of Sal B concentration in SM is approximately 5.0% of the root dry weight, which occupies approximately 70% of water-soluble phenolic acids extracted from SM, which is far higher than the concentration of Sal A in SM (30). Moreover, Sal B has been observed to be converted into Sal A under conditions of high temperature, high pressure and high humidity (31), which provides the possibility for united and continuous pharmacological activities resulting from Sal B-converted Sal A *in vivo*. The above findings hint that Sal B may have more potential and applied value than those of Sal A. However, Sal B has been only reported to inhibit A549 cell growth (12), while the pharmacological activity and the molecular mechanism of Sal B in regards to human NSCLC remain unsubstantiated. Therefore, Sal B was investigated to establish whether it possesses therapeutic properties against the human NSCLC A549 cell line via regulating TGF-β signaling. The results from the present study demonstrated that Sal B exhibited *in vitro* anticancer activity against NSCLC, which was reflected in the inhibition of A549 cell epithelial-mesenchymal transition (EMT), migration and cell cycle progression, the induction of cell autophagy and apoptosis-related inhibition of TGF-β signaling.

The occurrence and progression of NSCLC are closely involved in aberrant serial gene expression and numerous signaling pathways (32). Among these, TGF-β signaling serves a vitally important role in the patho-mechanism of NSCLC, as a result of its crosstalk with numerous molecules and signaling pathways, which results in the mediation of various cell biological behaviors (33,34). Therefore, TGF-β_1, a leading initiator of TGF-β signaling in mammals, was used in the present study to induce a human NSCLC progression model

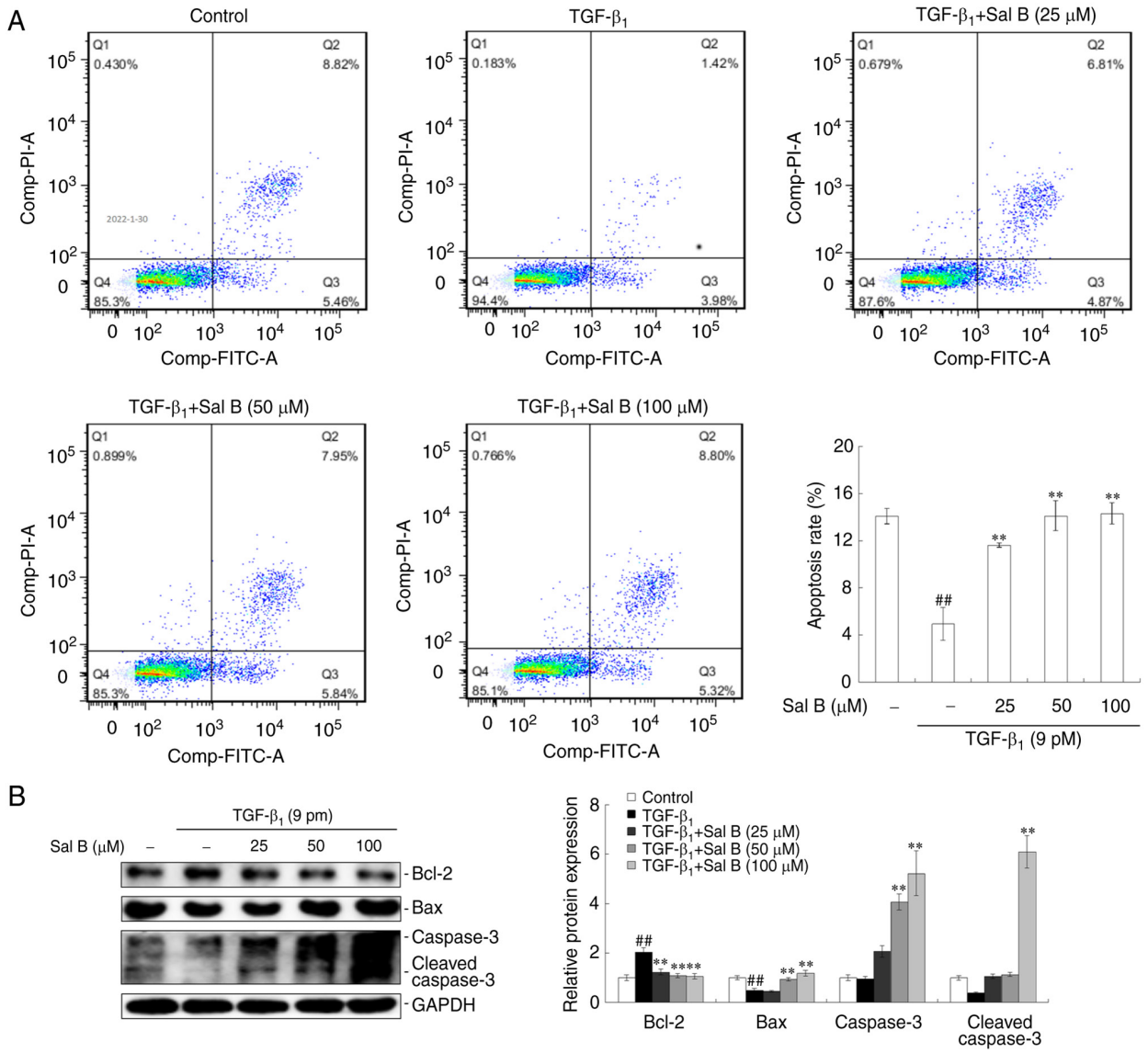

Figure 5. Effects of Sal B on cell apoptosis in TGF-β_1-stimulated A549 cells. (A) Cell apoptosis of A549 cells following treatment was assessed using the Annexin V-FITC/PI Double Dye Cell Apoptosis Detection kit. (B) Protein expression levels of cell apoptotic marker proteins, Bcl-2, Bax, caspase-3 and cleaved-caspase-3, were assessed via western blotting. $^{\#\#}$P<0.01 vs. the control; **P<0.01 vs. the TGF-β_1 only-stimulated group. Sal B, salvianolic acid B; TGF-β_1, transforming growth factor β_1.

in vitro in A549 cells prior to treatment with Sal B. The present study was therefore designed to investigate the effects of Sal B on human NSCLC progression via TGF-β signaling. The results demonstrated that TGF-β_1 was able to induce EMT, which was indicated by upregulated mesenchymal markers including N-cadherin, Vimentin and Snail, and downregulated epithelial marker E-cadherin. These changes simultaneously led to increased migration in A549 cells, whereas Sal B reversed these effects induced by TGF-β_1 and inhibited the EMT and migration of A549 cells. However, how Sal B intervenes in the process of EMT will be investigated in-depth in further research by using more experimental techniques such as observing cellular morphology under high-power microscope by immunofluorescent staining marked N-cadherin/E-cadherin in the near future. Furthermore, cell proliferation was inhibited by Sal B treatment, which was reflected by suppressed cell cycle progression and by the regulation of protein expression levels of critical markers, including cyclin B1 and p21 in TGF-β_1-stimulated A549 cells. Notably, the changes in Sal B-regulated cell cycle progression and its markers were found to be relatively weak in the present study, which may have resulted from the Sal B concentrations used which were less than its IC_{50} value in A549 cells (12). Unexpectedly, the protein level of cyclin B1 was slightly higher at 100 μM Sal B than that at 50 μM, which may have resulted from different regulatory mechanisms regarding the Sal B's concentration difference on cyclin B1 expression, considering that cyclin B1 has a dual face for regulating progression of the cell cycle (35). Subsequently, activation of cell autophagy and apoptosis by Sal B treatment were observed, which were indicated by Sal B-induced increased protein expression levels of autophagy marker proteins, LC3β and Beclin1 and decreased protein expression levels of p62. Yet, the mechanism regarding the influence of the entire process of A549 cell autophagy by Sal B requires further investigation. Further studies, including cell submicroscopic structure by using transmission electron microscopy, will be performed in the near future. Sal B induced

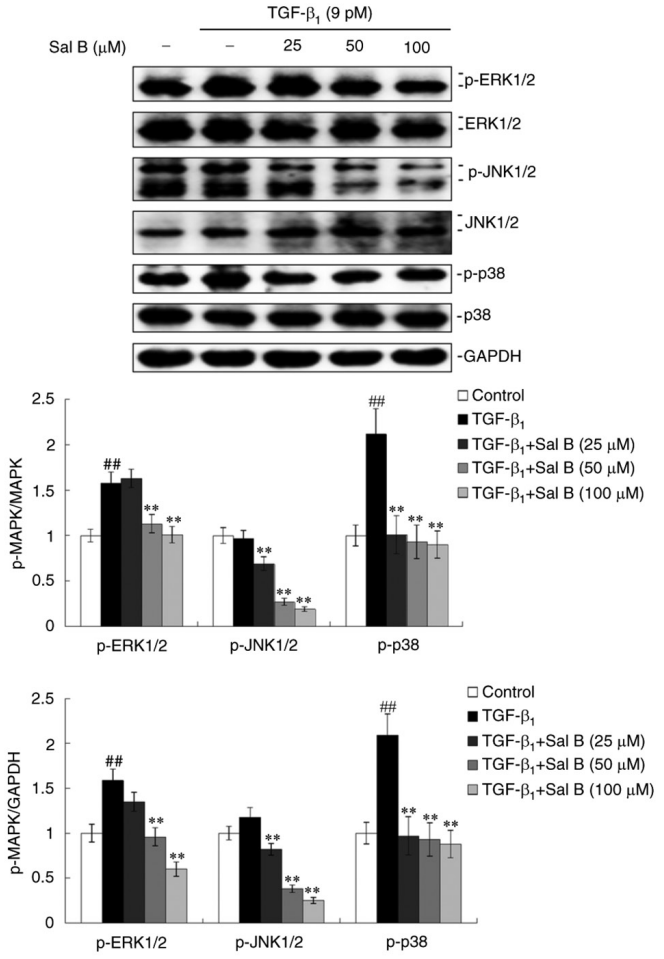

Figure 6. Effects of Sal B on the activation of MAPK signaling pathways in TGF-β_1-stimulated A549 cells. Protein expression levels of activated MAPKs, including p-ERK1/2, p-JNK1/2 and p-p38, and total MAPKs including ERK1/2, JNK1/2 and p38. were assessed via western blotting. $^{\#\#}$P<0.01 vs. the control; **P<0.01 vs. the TGF-β_1 only-stimulated group. Sal B, salvianolic acid B; p, phosphorylated; TGF-β_1, transforming growth factor β_1.

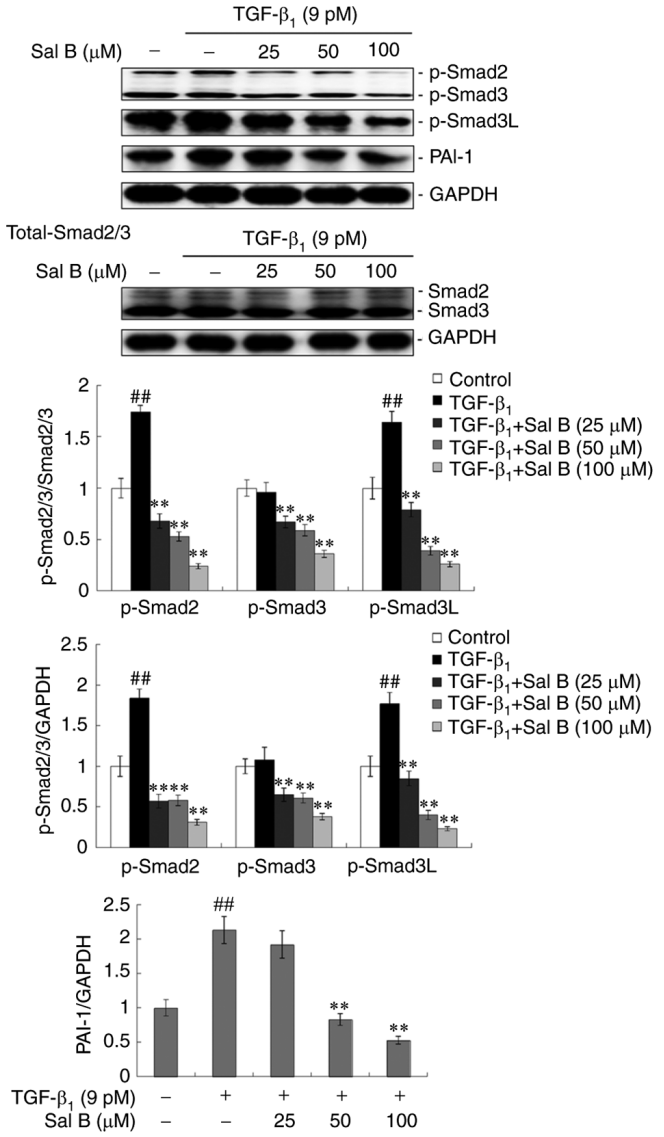

Figure 7. Effects of Sal B on the phosphorylation of Smad2/3 and the downstream target gene PAI-1 in TGF-β_1-stimulated A549 cells. Protein expression levels of p-Smad2/3, p-Smad3L, Smad2/3 and PAI-1, were assessed via western blotting. $^{\#\#}$P<0.01 vs. control; **P<0.01 vs. the TGF-β_1 only-stimulated group. Sal B, salvianolic acid B; PAI-1, plasminogen activator inhibitor-1; p, phosphorylated; L, linker region; TGF-β_1, transforming growth factor β_1.

increased apoptotic rates and protein expression levels of apoptotic marker proteins, including caspase-3/cleaved-caspase-3 and Bax, whereas protein expression levels of Bcl-2 were decreased. Numerous types of cancer cells, including NSCLC cells, have increased survival rates as a result of EMT, which is characterized by vigorous cell proliferation and migration and attenuated cell autophagy and apoptosis (36). The present study demonstrated that the *in vitro* anti-NSCLC efficacy of Sal B was reflected in the reduced cell EMT, migration and cell cycle progression, as well as activated autophagy and apoptosis via the TGF-β_1-induced human NSCLC progression model in A549 cells. Although the presented anticancer effects of Sal B on TGF-β_1-induced human NSCLC A549 progression were overall relatively weak in the study, this may have resulted from overactive TGF-β signaling in NSCLC itself and the used concentrations of Sal B much less than its IC_{50} value. Therefore, further research to investigate the effect of Sal B on NSCLC utilizing a more aggressive cell model to examine the intrinsic cause of the disease is required. For example, NSCLC cells with KRAS-mutations from lung cancer patients used for assessing the pharmacological activity of Sal B (37), which will be performed in the near future.

Moreover, the molecular mechanism of the anti-NSCLC effect of Sal B was investigated in the present study. The important role of TGF-β signaling in NSCLC and the inhibitory effects of Sal B on TGF-β_1-induced human NSCLC progression, resulted in the canonical and noncanonical TGF-β signaling pathways being analyzed to determine the association between Sal B and NSCLC. The canonical TGF-β signaling pathway is a Smad-dependent signaling pathway, which includes the following five stages. i) TGF-β_1, the dominating ligand of TGF-β signaling, attaches to the TGF-β receptor type II, located on the target cell membrane, and subsequently recruits and trans-phosphorylates TGF-β receptor type I (TβRI), located in the cytoplasm; ii) p-TβRI induces receptor-regulated Smad2/3 activation to produce p-Smad2/3; iii) p-Smad2/3 binds to the common mediator, Smad4, to produce heterotrimer/heterodimer

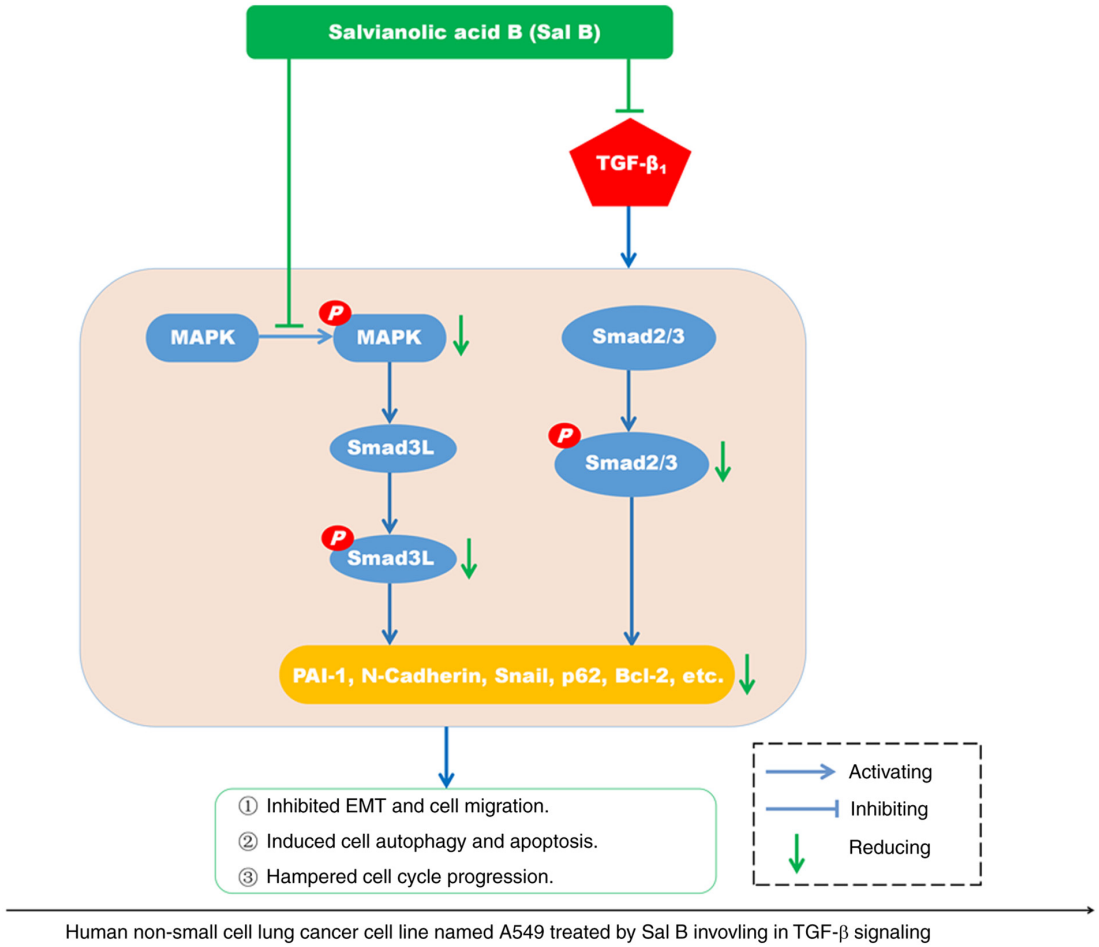

Figure 8. Schematic summary of the anti-NSCLC effect of Sal B in TGF-β signaling via inactivation of MAPK and phosphorylated (P)-Smad2/3 in A549 cells. NSCLC, non-small cell lung cancer; Sal B, salvianolic acid B; EMT, epithelial-mesenchymal transition; TGF-β, transforming growth factor β.

complexes, p-Smad2/3/4 or p-Smad3/4; iv) p-Smad2/3/4 and/or p-Smad3/4 are transported into the cell nucleus to regulate the expression of downstream target genes, including PAI-1, as a transcription factor; and v) inhibitory type Smad7 is transported into the nucleus to depolymerize p-Smad2/3/4 or p-Smad3/4, which results in the termination of TGF-β/Smad signal transduction (25). Smad2/3 phosphorylation is therefore an indispensable and central step for TGF-β/Smad signal transduction. The present study demonstrated that Sal B markedly inhibited TGF-β_1-induced Smad2/3 phosphorylation, which contributed to the inhibition of PAI-1 protein expression levels.

MAPK signaling pathways, noncanonical TGF-β signaling pathways, which include the ERK, JNK and p38 signaling pathways, are an attractive therapeutic target. Certain inhibitors of MEK have been used in an attempt to treat NSCLC by correcting aberrant MAPK signaling (38). In the present study, three MAPKs were assessed. The results demonstrated that Sal B markedly inhibited TGF-β_1-induced ERK1/2, JNK1/2 and p38 phosphorylation to reduce the activation of the ERK, JNK and p38 MAPK signaling pathways in A549 cells. For nearly 20 years, a series of studies from our research group and others have strongly suggested that Smad3 phosphorylation of Smad3L may be a crucial mechanism in TGF-β signaling, enabling a carcinogenic effect (26,39,40). Consequently, protein expression levels of p-Smad3L were assessed and the results demonstrated that Sal B decreased p-Smad3L protein expression levels in TGF-β_1-treated A549 cells. These results are supported by previous studies in which MAPK-regulated Smad2/3 phosphorylation has been demonstrated to enhance Smad2/3L phosphorylation via activated MAPK, which results in the occurrence and development of tumors and has been widely confirmed in keloid, HCC and colorectal cancer (18,41,42). PAI-1, an endogenous inhibitor of the urokinase-type plasminogen activator system, is induced by being directly bound to Smad3/Smad4, TGF-β-induced elements, at the PAI-1 promoter (43). Previous studies have reported that secreted PAI-1 increases EMT marker expression and enhances cell migration in *in vitro* and *in vivo* models of NSCLC (44,45). Extracellular PAI-1 activates the ERK1/2 and AKT signaling pathways and inhibits caspase-3 activity, which results in cell apoptosis inhibition in NSCLC (45). The present study observed that Sal B inhibited the ERK1/2 signaling pathway and Smad2/3 phosphorylation, which resulted in the inhibition of the downstream target gene PAI-1 and inhibited EMT and cell migration, whereas apoptosis was induced, in NSCLC A549 cells. However, whereas the characteristics of natural products have multiple target effects, Sal B maybe have multiple targets not only like-inhibitor of TGF-β signaling indicated in the study and/or disrupting of COX-2 activity reported previously in NSCLC (12). Therefore,

further research using NSCLC models *in vivo* and *in vitro* are required to investigate the underlying mechanisms of Sal B.

In summary, Sal B inhibited TGF-β_1-induced human NSCLC progression by inactivating the phosphorylation of MAPK and Smad2/3, which led to impeded TGF-β signaling transduction (Fig. 8). However, further research needs to be performed to determine the pharmacological efficacy of Sal B *in vivo* in NSCLC animal models or humans. Therefore, continued research into Sal B and other new therapeutics is urgently required. Animal models of NSCLC should be established and treated with suitable doses of Sal B to further support the potential clinical benefits of Sal B in patients with NSCLC, which may improve the survival rates and prognosis of patients with NSCLC.

Acknowledgements

Not applicable.

Funding

The present study obtained funding from the National Talent Project of Traditional Chinese Medicine Characteristic Technology Inheritance Supported National Administration of Traditional Chinese Medicine in China [no. 168 of Chinese Traditional Chinese Medicine Education Letter (2015)] and the National Natural Science Foundation of China (grant no. 81573652).

Availability of data and materials

The datasets used and/or analyzed during the current study are available from the corresponding author on reasonable request.

Authors' contributions

CW and YY conceptualized and designed the study. GH, YW, TL, FD and MC performed all experiments included in the study. GH, JG and CW contributed to the data collection, analysis, confirmed the authenticity of all the raw data and wrote the manuscript. CW and YY reviewed and edited the manuscript. GH and YY acquired funding. All authors have read and approved the final manuscript.

Ethics approval and consent to participate

Not applicable.

Patient consent for publication

Not applicable.

Competing interests

The authors declare that they have no competing interests.

References

1. Bade BC and Dela Cruz CS: Lung cancer 2020: Epidemiology, etiology, and prevention. Clin Chest Med 41: 1-24, 2020.
2. Herbst RS, Morgensztern D and Boshoff C: The biology and management of non-small cell lung cancer. Nature 553: 446-454, 2018.
3. Wang LC, Chang YY, Lee IC, Kuo HC and Tsai MY: Systematic review and meta-analysis of Chinese herbal medicine as adjuvant treatment in advanced non-small cell lung cancer patients. Complement Ther Med 52: 102472, 2020.
4. Chen X, Guo J, Bao J, Lu J and Wang Y: The anticancer properties of *Salvia miltiorrhiza* Bunge (Danshen): A systematic review. Med Res Rev 34: 768-794, 2014.
5. Hung YC, Pan TL and Hu WL: Roles of reactive oxygen species in anticancer therapy with *Salvia miltiorrhiza* Bunge. Oxid Med Cell Longev 2016: 5293284, 2016.
6. Gong L, Di C, Xia X, Wang J, Chen G, Shi J, Chen P, Xu H and Zhang W: AKT/mTOR signaling pathway is involved in salvianolic acid B-induced autophagy and apoptosis in hepatocellular carcinoma cells. Int J Oncol 49: 2538-2548, 2016.
7. Katary MA, Abdelsayed R, Alhashim A, Abdelhasib M and Elmarakby AA: Salvianolic acid B slows the progression of breast cancer cell growth via enhancement of apoptosis and reduction of oxidative stress, inflammation, and angiogenesis. Int J Mol Sci 20: 5653, 2019.
8. Hao Y, Xie T, Korotcov A, Zhou Y, Pang X, Shan L, Ji H, Sridhar R, Wang P, Califano J and Gu X: Salvianolic acid B inhibits growth of head and neck squamous cell carcinoma in vitro and in vivo via cyclooxygenase-2 and apoptotic pathways. Int J Cancer 124: 2200-2209, 2009.
9. Chen B, Huang C, Zhang Y, Tang X, Li S, Wang Q and Lin Y: *Salvia bowleyana* Dunn root is a novel source of salvianolic acid B and displays antitumor effects against gastric cancer cells. Oncol Lett 20: 817-827, 2020.
10. Jing Z, Fei W, Zhou J, Zhang L, Chen L, Zhang X, Liang X, Xie J, Fang Y, Sui X, *et al*: Salvianolic acid B, a novel autophagy inducer, exerts antitumor activity as a single agent in colorectal cancer cells. Oncotarget 7: 61509-61519, 2016.
11. Qin T, Rasul A, Sarfraz A, Sarfraz I, Hussain G, Anwar H, Riaz A, Liu S, Wei W, Li J and Li X: Salvianolic acid A & B: Potential cytotoxic polyphenols in battle against cancer via targeting multiple signaling pathways. Int J Biol Sci 15: 2256-2264, 2019.
12. Tao L, Wang S, Zhao Y, Sheng X, Wang A, Zheng S and Lu Y: Phenolcarboxylic acids from medicinal herbs exert anticancer effects through disruption of COX-2 activity. Phytomedicine 21: 1473-1482, 2014.
13. Dongre A and Weinberg RA: New insights into the mechanisms of epithelial-mesenchymal transition and implications for cancer. Nat Rev Mol Cell Biol 20: 69-84, 2019.
14. Jeong JH, Jang HJ, Kwak S, Sung GJ, Park SH, Song JH, Kim H, Na Y and Choi KC: Novel TGF-β1 inhibitor antagonizes TGF-β1-induced epithelial-mesenchymal transition in human A549 lung cancer cells. J Cell Biochem 120: 977-987, 2019.
15. Eser PÖ and Jänne PA: TGFβ pathway inhibition in the treatment of non-small cell lung cancer. Pharmacol Ther 184: 112-130, 2018.
16. Liu Q, Chu H, Ma Y, Wu T, Qian F, Ren X, Tu W, Zhou X, Jin L, Wu W and Wang J: Salvianolic acid B attenuates experimental pulmonary fibrosis through inhibition of the TGF-β signaling pathway. Sci Rep 6: 27610, 2016.
17. Wu C, Chen W, Ding H, Li D, Wen G, Zhang C, Lu W, Chen M and Yang Y: Salvianolic acid B exerts anti-liver fibrosis effects via inhibition of MAPK-mediated phospho-Smad2/3 at linker regions in vivo and in vitro. Life Sci 239: 116881, 2019.
18. Boye A, Kan H, Wu C, Jiang Y, Yang X, He S and Yang Y: MAPK inhibitors differently modulate TGF-β/Smad signaling in HepG2 cells. Tumour Biol 36: 3643-3651, 2015.
19. Hao Y, Baker D and Ten Dijke P: TGF-β-mediated epithelial-mesenchymal transition and cancer metastasis. Int J Mol Sci 20: 2767, 2019.
20. Liu X, Chen Y, Li Y, Petersen RB and Huang K: Targeting mitosis exit: A brake for cancer cell proliferation. Biochim Biophys Acta Rev Cancer 1871: 179-191, 2019.
21. Mateen S, Raina K, Jain AK, Agarwal C, Chan D and Agarwal R: Epigenetic modifications and p21-cyclin B1 nexus in anticancer effect of histone deacetylase inhibitors in combination with silibinin on non-small cell lung cancer cells. Epigenetics 7: 1161-1172, 2012.
22. Liu G, Pei F, Yang F, Li L, Amin AD, Liu S, Buchan JR and Cho WC: Role of autophagy and apoptosis in non-small-cell lung cancer. Int J Mol Sci 18: 367, 2017.
23. Kim R, Emi M and Tanabe K: The role of apoptosis in cancer cell survival and therapeutic outcome. Cancer Biol Ther 5: 1429-1442, 2006.

24. Mulder KM: Role of Ras and Mapks in TGFbeta signaling. Cytokine Growth Factor Rev 11: 23-35, 2000.
25. Derynck R and Zhang YE: Smad-dependent and Smad-independent pathways in TGF-beta family signalling. Nature 425: 577-584, 2003.
26. Ooshima A, Park J and Kim SJ: Phosphorylation status at Smad3 linker region modulates transforming growth factor-β-induced epithelial-mesenchymal transition and cancer progression. Cancer Sci 110: 481-488, 2019.
27. Zhou Y, Zheng J, Li Y, Xu DP, Li S, Chen YM and Li HB: Natural polyphenols for prevention and treatment of cancer. Nutrients 8: 515, 2016.
28. Bi L, Chen J, Yuan X, Jiang Z and Chen W: Salvianolic acid A positively regulates PTEN protein level and inhibits growth of A549 lung cancer cells. Biomed Rep 1: 213-217, 2013.
29. Tang XL, Yan L, Zhu L, Jiao DM, Chen J and Chen QY: Salvianolic acid A reverses cisplatin resistance in lung cancer A549 cells by targeting c-met and attenuating Akt/mTOR pathway. J Pharmacol Sci 135: 1-7, 2017.
30. Sun Y, Zhu H, Wang J, Liu Z and Bi J: Isolation and purification of salvianolic acid A and salvianolic acid B from *Salvia miltiorrhiza* by high-speed counter-current chromatography and comparison of their antioxidant activity. J Chromatogr B Analyt Technol Biomed Life Sci 877: 733-737, 2009.
31. Xia H, Sun L, Lou H and Rahman MM: Conversion of salvianolic acid B into salvianolic acid A in tissues of radix salviae miltiorrhizae using high temperature, high pressure and high humidity. Phytomedicine 21: 906-911, 2014.
32. Petty RD, Nicolson MC, Kerr KM, Collie-Duguid E and Murray GI: Gene expression profiling in non-small cell lung cancer: From molecular mechanisms to clinical application. Clin Cancer Res 10: 3237-3248, 2004.
33. Jeon HS and Jen J: TGF-beta signaling and the role of inhibitory Smads in non-small cell lung cancer. J Thorac Oncol 5: 417-419, 2010.
34. Wang J, Shao N, Ding X, Tan B, Song Q, Wang N, Jia Y, Ling H and Cheng Y: Crosstalk between transforming growth factor-β signaling pathway and long non-coding RNAs in cancer. Cancer Lett 370: 296-301, 2016.
35. Schnittger A and De Veylder L: The dual face of cyclin B1. Trends Plant Sci 23: 475-478, 2018.
36. Mittal V: Epithelial mesenchymal transition in aggressive lung cancers. Adv Exp Med Biol 890: 37-56, 2016.
37. Calles A, Sholl LM, Rodig SJ, Pelton AK, Hornick JL, Butaney M, Lydon C, Dahlberg SE, Oxnard GR, Jackman DM and Jänne PA: Immunohistochemical loss of LKB1 is a biomarker for more aggressive biology in KRAS-mutant lung adenocarcinoma. Clin Cancer Res 21: 2851-2860, 2015.
38. Kim C and Giaccone G: MEK inhibitors under development for treatment of non-small-cell lung cancer. Expert Opin Investig Drugs 27: 17-30, 2018.
39. Murata M, Yoshida K, Yamaguchi T and Matsuzaki K: Linker phosphorylation of Smad3 promotes fibro-carcinogenesis in chronic viral hepatitis of hepatocellular carcinoma. World J Gastroenterol 20: 15018-15027, 2014.
40. Gong Y, Li D, Li L, Yang J, Ding H, Zhang C, Wen G, Wu C, Fang Z, Hou S and Yang Y: Smad3 C-terminal phosphorylation site mutation attenuates the hepatoprotective effect of salvianolic acid B against hepatocarcinogenesis. Food Chem Toxicol 147: 111912, 2021.
41. He S, Liu X, Yang Y, Huang W, Xu S, Yang S, Zhang X and Roberts MS: Mechanisms of transforming growth factor beta(1)/Smad signalling mediated by mitogen-activated protein kinase pathways in keloid fibroblasts. Br J Dermatol 162: 538-546, 2010.
42. Matsuzaki K, Kitano C, Murata M, Sekimoto G, Yoshida K, Uemura Y, Seki T, Taketani S, Fujisawa J and Okazaki K: Smad2 and Smad3 phosphorylated at both linker and COOH-terminal regions transmit malignant TGF-beta signal in later stages of human colorectal cancer. Cancer Res 69: 5321-5330, 2009.
43. Dennler S, Itoh S, Vivien D, ten Dijke P, Huet S and Gauthier JM: Direct binding of Smad3 and Smad4 to critical TGF beta-inducible elements in the promoter of human plasminogen activator inhibitor-type 1 gene. EMBO J 17: 3091-3100, 1998.
44. Lin X, Lin BW, Chen XL, Zhang BL, Xiao XJ, Shi JS, Lin JD and Chen X: PAI-1/PIAS3/Stat3/miR-34a forms a positive feedback loop to promote EMT-mediated metastasis through Stat3 signaling in non-small cell lung cancer. Biochem Biophys Res Commun 493: 1464-1470, 2017.
45. Kang J, Kim W, Kwon T, Youn H, Kim JS and Youn B: Plasminogen activator inhibitor-1 enhances radioresistance and aggressiveness of non-small cell lung cancer cells. Oncotarget 7: 23961-23974, 2016.